EUROPEAN ORGANIZATION FOR NUCLEAR RESEARCH

10 April, 1967

P R O P O S A L

To : EEC

From : W. Kienzle, C. Lechanoine*), B. Maglić (CERN)**),
G. Chikovani (Georgian Academy of Science, Tbilisi, USSR),
M.N. Focacci, B. Levrat, M. Martin (University of Geneva),
P. Schübelin (University of Bern).

Subject : Magnetic boson spectrometer for masses up to 4 GeV

CONTENTS

---

*) On leave from Faculté des Sciences, Paris.

**) E. Zavattini and R. Rigopoulos (Institute "Democritus", Athens) will help in setting up and operating a neutron spectrometer for $\pi^+ p \to n X^{++}$ (T = 2) bosons in the second phase of the experiment, once the main spectrometer is running.

1. INTRODUCTION

We propose a systematic study of the spectrum of non-strange bosons X^- produced in $\pi^- p \to pX^-$ in the mass range $2 < M_X < 4$ GeV, using incident pion momenta between 6 and 18 GeV/c. This is, with a new method, an extension to higher masses of our earlier work on mesons, shown in Fig. 0. A magnetic spectrometer operating at 0° lab. angle and consisting of a wide-gap magnet, sonic and wire spark chambers with an on-line computer, does the following measurements:

- magnetic analysis of the forward emitted proton, which gives the mass of X^- by the method of missing mass with very good resolution;
- number and direction of the charged decay products of X^-;
- effective mass of X^- for decays into three charged pions.

The system is ready and, apart from the magnet, has been operated successfully in production runs in the former MM experiment, where a different method was used ("Jacobian peaks") which cannot be applied to masses > 2.5 GeV with existing beams. The magnet is at present being mapped.

2. METHOD

In the lab. system, the angle ϑ and momentum p_3 of the recoil proton in the reaction

$$\underset{1}{\pi^-} + \underset{2}{p} \to \underset{3}{p} + \underset{4}{X^-}$$

are related, for given mass of X^- and a given p_1 as shown on Fig. 1, where

$$M_X^2 = (E_1 + m_2 - E_3)^2 - p_1^2 - p_3^2 + 2p_1 p_3 \cos\vartheta \ .$$

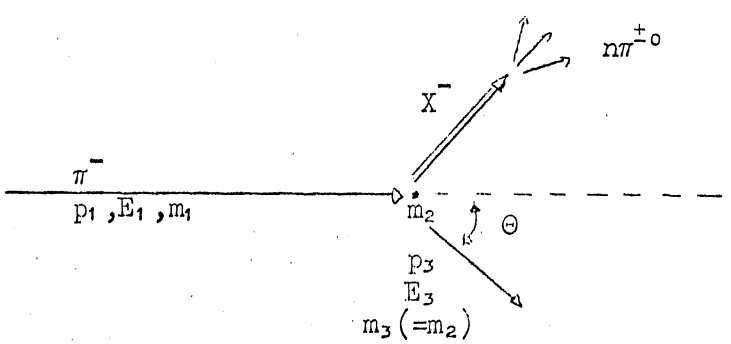

The method considered here is to measure p_3 and ϑ_3 in region II. In the centre-of-mass system, this corresponds to forward production of X^-, i.e. the proton going backwards. In this region, the mass resolution is determined essentially by the accuracy of p_3, while the measurement of ϑ is not critical. (This is the opposite of the "Jacobian peak method" of the former MM experiment.)

The main features of the method are the following:

- masses up to 4 GeV can be reached with beams at present available at the PS (for a given p_1, M_X is 1-1.5 GeV higher than with the "Jacobian peak method");
- a given mass is measured at its lowest kinematically possible momentum transfer, therefore highest differential production cross-section, (which is at 0° and for a given mass by at least a factor 1000 larger than at the corresponding "Jacobian peak");
- the mass resolution is between 10 and 20 MeV (full width) and only weakly mass dependent;
- the trigger rate is high enough to saturate the system, i.e. at least 15 events per burst.

Simultaneously with the measurement of p_3 and ϑ_3, the number and direction of the charged products of X^- are measured. In the case of three charged pions this allows the reconstruction of the effective mass, and the possible determination of spin and parity from angular correlations and Dalitz plot analysis. (A Dalitz plot of the A_2 meson has already been obtained with the wire chambers of Fig. 2 in January 1967, showing the ρ in the projections.)

A comparison between the here proposed "0° method" and the "Jacobian peak method" is given in Table 1 for different values of incident momentum p_1 and mass M_X.

NOTE: The 0° method has been used at Brookhaven by Hyman et al. in $\pi^- p \to n X^0$, where they measured the neutron momentum by time-of-flight. A strong η was obtained, sitting on only 15% background.

Table 1

Mass bites and resolutions

p_1 = 6, 12, 18 GeV/c ($\Delta p_1/p_1$ = 1%); p_3 = 0.35 - 0.90 GeV/c ($\Delta p_3/p_3$ = 1%)

p_1 (GeV/c)	c.m. E_{max} (GeV)	Jacobian peak method		Magnetic spectrometer	
		M_X(GeV)	Γ_{exp}	M_X(GeV)	Γ_{exp}
6	2.5	1.30 0.85 - 1.55	± 13 MeV	2.10 1.80 - 2.40	± 6 MeV
12	3.9	1.90 1.40 - 2.30	± 12 MeV	3.10 2.7 - 3.5	± 9 MeV
18	5.0	2.20 1.40 - 2.70	± 12 MeV	3.80 3.3 - 4.3	± 11 MeV

3. THE INSTRUMENT

3.1 Technical equipment

The laboratory momentum p_3 of the recoil proton (i.e. the missing-mass M_X) is measured with a magnetic spectrometer (Fig. 2) consisting of points (i) to (iv) :

i) Two magnetostrictive wide-gap chambers VC1 and VC2

The wire chambers have been operated successfully in January 1967 for two weeks. They each consist of two crossed planes of wires, with 150 × 150 cm² fiducial area, 10 cm gap, 1 mm wire spacing. A report about their properties and performance will be given to the EEC on 17 April, 1967.

ii) A wide-gap magnet

The magnet considered is magnet No. 2 of the NP Division (gap : 0.5 × 1.0 × 1.5 m³, operated at 12 kG). This magnet is at present being tested and mapped by the NP Magnet Group.

iii) Four acoustic spark chambers

The acoustic chambers are the same as in the former MM experiment, and have been operated without difficulties for more than one year.

iv) A trigger system to select protons (for description, see below)

The scintillators and fast logics are available from the former MM experiment, with only minor modifications necessary.

The decay products of X^- are measured simultaneously with the proton with the wide-gap wire chambers described under point (i).

For data acquisition we will use an IBM 1800 computer, which does the sampling of events and writes magnetic tapes. The computer will be available from the University of Geneva.

3.2 Proton spectrometer

3.2.1 Identification of protons. Protons and pions coming from the target are distinguished by the time-of-flight over a distance of about 5 metres in the trigger condition. Figure 3 shows the time-of-flight spectrum obtained by a Monte Carlo calculation for protons and pions, with a field of 12 kG and a lower limit of p_3 of 0.35 GeV/c, given by range.

The rejection level of pions is $\geq 99\%$ with a $p_3^{max} = 0.900$ GeV/c, assuming a geometric plus electronic spread in the time-of-flight of 6.5 nsec. For kaons, a similar contamination is obtained under the same conditions.

This technique has been used for more than one year in the former MM experiment, with more pion background, since no magnetic field was available.

3.2.2 Rejection of "simultaneous" pions. In 14% of cases, the proton is accompanied by a pion coming from the decay of X^-, or phase space of mass M_X. However, these pions cannot produce a trigger since they are faster than the associated proton, so that the system is still

dead when the proton arrives. (The R1 counter operates with 50 nsec dead-time in its shaper, and the protons are 10 - 20 nsec late with respect to associated pions.) The proton telescope will therefore trigger only on single tracks in the sonic chambers. This means that their replacement by wire chambers would have no advantages.

3.2.3 Distinction between pion and proton tracks in the wire chambers. Detailed Monte Carlo estimates have been made to check how well the proton tracks can be distinguished from pion tracks in the wire chambers. In 98% of the cases, a proton track can be reconstructed unambiguously. Figure 4 shows the distribution of the separation between a reconstructed proton track and measured positions in chamber 1, using pion and proton tracks in chamber 2, and the proton tracks from the sonic chambers. The sharp spike of zero arises from protons, the flat continuum from pions.

From points 3.2.1 to 3.2.3 above, it is concluded that a clean, i.e. $\geq$ 97%, proton sample can be obtained, and the momentum measured.

3.2.4 Shape of the mass spectrum. The detection probability for a recoil proton coming from the target, as a function of mass M_X and p_3, has been determined by Monte Carlo methods. We used as input a flat mass spectrum with differential cross-section $d\sigma/d|t|$ proportional to $e^{-8|t|}$ for $0.3 \leq p_3 \leq 1.5$ GeV/c, and $p_1 = 12$ GeV/c.

The output of the spectrometer is presented in Fig. 5, and shows that the spectrum is quite smooth, and a peak superimposed on this background can therefore be distinguished. The total detection probability (ratio of detected to produced protons) is 4.6% in the mass range given above.

3.2.5 Mass resolution. The mass resolution is given by $\Gamma^{\text{total}} = \{\Gamma_{p_1}^2 + \Gamma_{p_3}^2 + \Gamma_\vartheta^2\}^{\frac{1}{2}}$ where Γ_ϑ is negligibly small since $dM/d\vartheta = 0$ at $\vartheta = 0°$, and where :

$$\Gamma_{p_1} = \frac{p_3 \cos\vartheta - \beta_1 T_3}{M_X} \Delta p_1 \ , \quad \Gamma_{p_3} = \frac{p_1 \cos\vartheta - \beta_3 E_0}{M_X} \Delta p_3 \ .$$

The contributions from Γ_{p_1} and Γ_{p_3} are about equal. The uncertainty on p_1 is taken as 1%, as justified from our experience in the d beam. The value of $\Delta p_3/p_3$ has been taken as 1%, which comes equally from multiple scattering

(5.7 mrad at p_3 = 0.5 GeV/c) and spatial resolution (5.3 mrad) due to wire spacing in the chambers. The accuracy of the magnetic field mapping is assumed to be 2‰.

The energy loss of the proton on its path through the hydrogen of the target has been studied in detail. We find that the contribution to Γp_3 coming from an uncertainty in this energy loss is negligible, compared to Γp_3 coming from the magnetic spectrometer. The reason is that the vertex, and therefore the path length of the proton in hydrogen, are well known (vertex to ± 4 mm) due to vertex reconstruction with the decay pions.

The total experimental resolution is shown in Fig. 6 as a function of p_1 and M_X. A typical value is Γ^{exp} = 18 MeV (full width at half maximum).

3.3 Decay analysis

The number of charged decay products and their directions are obtained from the wire chambers VC1 and VC2. The trigger accepts events only if all charged decay products are going into the chambers. These chambers can handle five sparks with at least 95% efficency.

The acceptance of the two wire chambers for three-pion decays of X^- as a function of p_1 and M_X is shown in Fig. 7. It is seen that for $9 < p_1 < 18$ GeV/c and $2 < M_X < 4$ GeV, in more than 70% of the events with a good proton all three decay pions are going into the solid angle defined by the wire chambers. We do not consider it worth while to put more chambers around the target in order to increase the solid angle, since the trigger rate is already high enough to saturate the data system. From Monte Carlo calculations we find that four more wire chambers sideways around the target would increase the three-pion acceptance by only 10-15%.

The effective mass can be contructed in cases where X^- decays into three charged pions only. Knowing the three directions of these pions, their momenta can be calculated, since we have four equations from four-momentum conservation and three unknowns only. We have therefore a one-constraint fit, which allows the elimination of π^o's.

This method has been used successfully in the case of the A_2 meson in January, 1967, using the wire chambers of Fig. 2. The difference between three-pion effective mass thus obtained and the simultaneously measured MM is shown in Fig. 8, this difference being typically ± 30 MeV.

Details about this method will be presented to the EEC on 17 April, 1967.

3.4 Trigger and data system

3.4.1 Trigger condition. A simplidied fast logics diagram is shown in Fig. 9a.

The trigger conditions are

a) incoming particle and interaction in target - H1 H2 T $\bar{B}$ V $\bar{V}$;

b) recoil proton in proper angular and momentum range R1 R2 $\overline{R3}$.

We estimate the accidental triggers to be below 10%. A system of anti-counters $\bar{V}$ around the backward hemisphere of the target allows the trigger only when all charged decay products of X^- go into the wire chambers.

3.4.2 Data acquisition (see Fig. 9b). The whole information of each event is digitized into 100 scalers, pattern units, and parameter units. For the sonic and wire chambers we use the first 16 bits of fast (25 Mc) 24-bit scalers. After each event they are read into the memory of the IBM 1800, from whence the information goes in blocks of 15 events on magnetic tape. The reading time of the 100 scalers in small compared to the 10 msec chamber dead-time. No filtering can be done before writing on tape. One event per PS burst can be sampled and analysed on-line in some detail. Twice a day we analyse tapes of 30-50,000 events off-line on the CDC 3800 ("bicycle ON-LINE"). On-line operation with a big computer (e.g. CDC 6600) worked well in our runs with the former MM experiment, and would also be desirable in the production runs of this experiment.

3.4.3 Event rate and statistical sensitivity. We obtain one trigger per 10^3 incident pions, taking a target length of 50 cm and taking a total cross-section of 10 mb for the reaction $\pi^- p \to pX^-$, at 12 GeV/c. This gives us us 3×10^5 triggers per day, assuming 7×10^4 incident pions per burst, and the beam working 70% of the time.

Fifteen triggers per burst are accepted by our system, the limitation coming from the 10 msec dead-time of the spark chambers.

From experience with the former MM system, we know that this gives 6×10^4 good events per day in the final histograms, in a mass bite of 600 MeV width. Therefore, in order to establish the existence of a narrow resonance of 10 μb total cross-section with a statistical significance of 6 standard deviations, we need two new PS weeks of running.

3.4.4 Off-line computing. Since the full analysis will be done off-line (except, if a big on-line facility is available permanently) we need the following amount of CDC 3800 (or equivalent) time (see also section 4, Table 2) :

i) Technical runs

1967 (Sept. - Dec.) 2 × 30 h with priority, distributed over 2 × 2 new PS weeks (i.e. over 6 computer weeks)

+ 2 × 90 h without priority, distributed over the same time.

ii) Test run

1968 (Jan. - March) 1 × 75 h with priority, distributed over 2 new PS weeks

+ 1 × 150 h without priority, distributed over 2 new PS weeks

+ 100 h for SUMX, over the same period.

The last block corresponds to a production run of 2 new PS weeks, and would be repeated five times (PRODUCTION RUNS 1 - 5) in addition to this test run in 1968.

4. SCHEDULE OF RUNS

Table 2

Type of run	Subject	Beam momentum		Intensity (per $\frac{\Delta p_t}{p_t} = 1\%$)	PS time	Date
Technical Run No. 1	Setting up	$\gtrsim 4$ GeV/c	π^+	$> 10^4$	2 new PS weeks	Sept. Oct. 1967
Technical Run No. 2	Elastic test	4 GeV/c	π^-	$> 2 \times 10^4$	"	Nov. Dec. 1967
Test run	R meson	4.0 GeV/c	π^-	$\approx 10^5$	"	Jan. Feb. 1968
Production Run No. 1	1.8-2.4 GeV	6.0 GeV/c	"	"	2 new PS weeks	
No. 2	2.3-3.0	9.0 GeV/c	"	"	"	
No. 3	2.7-3.5	12.0 GeV/c	"	"	"	
No. 4	2.9-3.8	15.0 GeV/c	"	?	"	
No. 5	3.3-4.3	18.0 GeV/c	"	?	"	

5. FURTHER EXPERIMENTAL PROGRAM

As soon as the boson spectrometer is running in the form described above, three extensions can be made.

5.1 Doubly charged bosons (T = 2) in the reaction $\pi^+ p \to nX^{++}$

A π^+ beam would be used instead of π^- to investigate :

i) with the proton spectrometer, the spectrum of X^+ which is equivalent to X^- ($T = 1$ or 2, $T_z = 1$) in the reaction $\pi^+ p \to pX^+$, and simultaneously :

ii) with a neutron spectrometer, operating at the "Jacobian peak", the spectrum of X^{++} ($T = 2$, $T_z = 2$) in $\pi^+ p \to nX^{++}$.

The question whether $T = 2$ bosons exist is of fundamental importance for the classification of elementary particles, e.g. the Dalitz quark model. The neutron detector would be built and operated by E. Zavattini and R. Rigopoulos. The upper mass limit for $M_{X^{++}}$ would be 2.7 GeV.

5.2 Detection of π^0's in the decay of $X^{\pm}$ (or X^{++}, respectively)

As the next step, automatic γ-sensitive wire chambers would be set up around the target, subtending the same solid angle as our wire chambers. At the same time, the trigger should be arranged in such a way that events are accepted only if all (i.e. $\pi^{\pm}$ and π^0's) decay products of $X^{\pm}$, X^{++} go into the combined charge and neutral sensitive chambers (by making $\bar{V}$ γ-sensitive). Thus the branching ratios of singly and (if they exist) doubly charged bosons into charged and neutral particles would be measured.

The CERN-Trieste Group, for example, which is at present developing γ-sensitive wire chambers, has expressed a strong interest in associating their equipment (once it is ready for production runs) with our main spectrometer.

5.3 Bosons of very high mass, up to 8 GeV : Serpukhov

The magnetic boson spectrometer would be well suited to run in one of Serpukhov's secondary pion beams for masses of $X^{\pm}$ up to $M_X = 8$ GeV with a resolution of $\pm$ 15 MeV, quite independent of mass, using incident pion momenta p_1 = 30-60 GeV/c.

In more than 90% of the cases, all decay products of $X^{\pm}$ would be accepted by our two forward wire chambers, in the arrangement described above.

A detailed study of this subject has been made, and a memorandum was submitted to A. Wetherell, on 20 February, 1967.

Figure captions

Fig. 0 : Compiled spectrum of bosons, measured in the reaction $\pi^- p \to pX^-$ with the former missing-mass spectrometer [Phys.Rev.Letters 17, 890 (1966)]. A tentative extrapolation to masses above 2,5 GeV of the straight line which fits well the squared boson masses in the known region, may suggest what one could expect to find with the new magnetic boson spectrometer.

Fig. 1 : Kinematics for $\pi^- + p \to p\, X^-$ with $p_1 = 12.0$ GeV/c for different values of M_X.

Heavy rectangular boxes :
I) "Jacobian peak method" at low masses
II) "0° method"
III) "Jacobian peak method" at high masses.

To demonstrate the avantages of the "0° method" at high masses.

Fig. 2 : Experimental layout of the magnetic boson spectrometer

Fig. 3 : Distinction of protons from pions
Time-of-flight distributions of protons and pions over a distance of 5 metres from the target through the magnet (12.0 kG) to the R1 counter. The time separation of 6.5 nsec between p and π takes into account geometric and electronic spreads in the time-of-flight measurement.

Fig. 4 : Distinction (in space) between proton and pion tracks in the wire chambers with the help of track reconstruction through the magnetic field.

Single tracks in the sonic chambers are combined with any track in wire chamber 2 (be it a pion or a proton), and extrapolated into wire chamber 1. There the difference is taken between the extrapolated and all measured tracks. The number of events is shown as a function of this difference : it is seen that protons (narrow peak near 0) are well distinguished from pions (flat background), the pion contamination being only 2%.

Fig. 5 : Shape of mass spectrum as obtained from magnetic analysis of the recoil proton around 0° lab. angle (i.e. a missing mass spectrum). A flat mass spectrum has been used as input, with $d\sigma/dt \sim e^{-8|t|}$, and p_1 = 12 GeV/c. The parameters of the actual set-up (Fig. 2) were used. The upper limit in M_X is given by the limit in p_3, which itself is determined by the separations of protons from pions through time-of-flight. [The envelope (heavy line) is for $0.3 < p_3 \leq 1.5$ GeV/c.]

Fig. 6 : Mass resolution of proton spectrometer as a function of incident momentum p_1 and missing mass M_X.

Parameters $\Delta p_1/p_1 = 1\%$, $\Delta p_3/p_3 = 1\%$, $\vartheta = 0°$ ($\vartheta = \pm 10°$ gives only negligible contributions).

Fig. 7. : Percentage of cases where all three charged decay products of X^- are accepted by the wire chambers, as a function of p_1 and M_X. The circles indicate the average mass M_X at which the spectrometer would operate for a given p_1. For decay multiplicities higher than 3, the acceptance increases, since the Q-value decreases for a given M_X.

Fig. 8 : Comparison between effective mass M_{eff}, as measured by the wire chambers in the case of three charged decay pions of X^-, with the missing mass M_X, as measured simultaneously by the proton spectrometer. The number of events is shown as a function of the difference $M_{eff} - M_X$; this is not from Monte Carlo calculation, but a result of our production on the A_2 meson in January 1967.

Fig. 9 : Trigger and data system :

a) simplified fast logics diagram, to demonstrate how a trigger is obtained;
b) data acquisition and treatment (schematic).

fig. 0

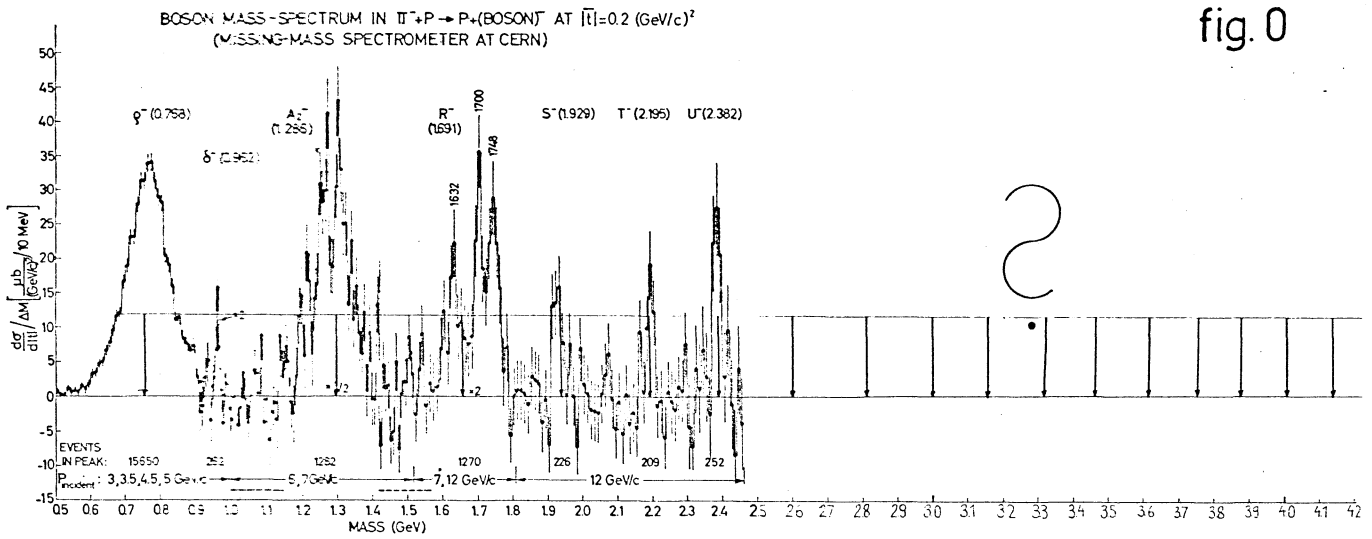
BOSON MASS-SPECTRUM IN π⁻+P → P+(BOSON)⁻ AT |t|=0.2 (GeV/c)²
(MISSING-MASS SPECTROMETER AT CERN)
ρ⁻(0.758)
δ⁻(0.962)
A₂⁻ (1.286)
R⁻ (1691)
1632
1700
1748
S⁻(1.929)
T⁻(2.195)
U⁻(2.382)
EVENTS IN PEAK: 15650 252 1262 1270 226 209 252
P incident: 3,35,4,5,5 GeV/c — 5,7GeV/c — 7,12 GeV/c — 12 GeV/c
MASS (GeV)

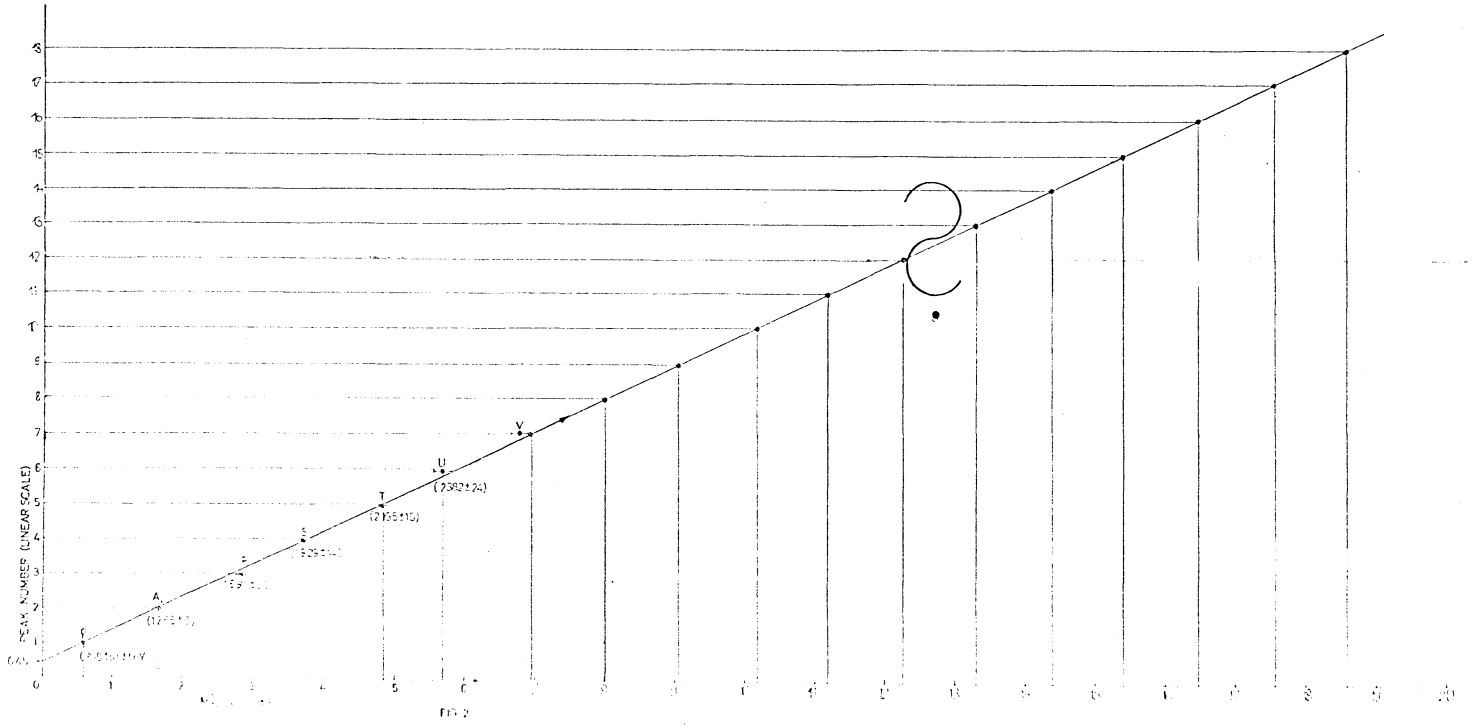
PEAK NUMBER (LINEAR SCALE)
S
A
T
U
V

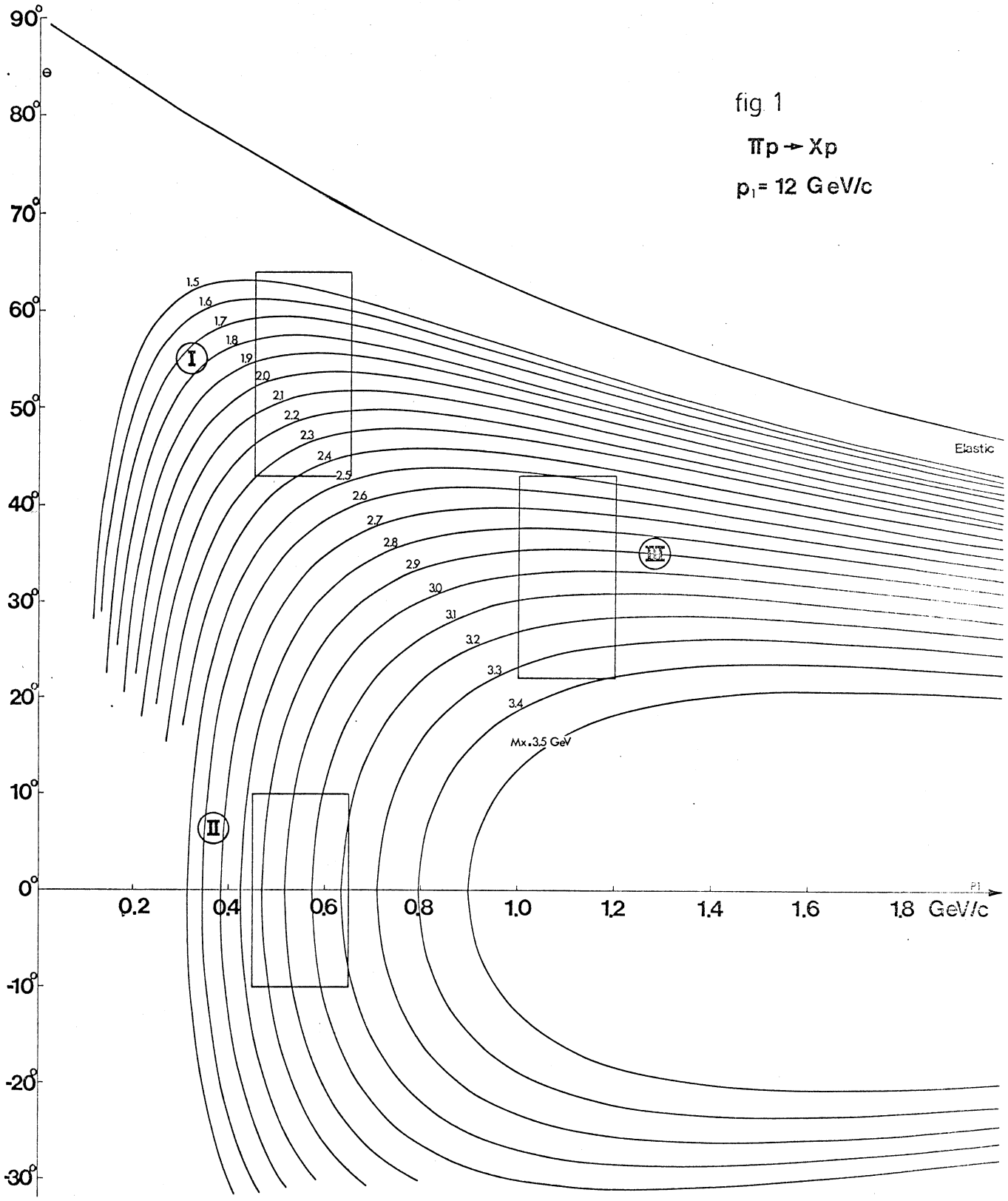

fig. 1

$\pi p \rightarrow Xp$

$p_1 = 12$ GeV/c

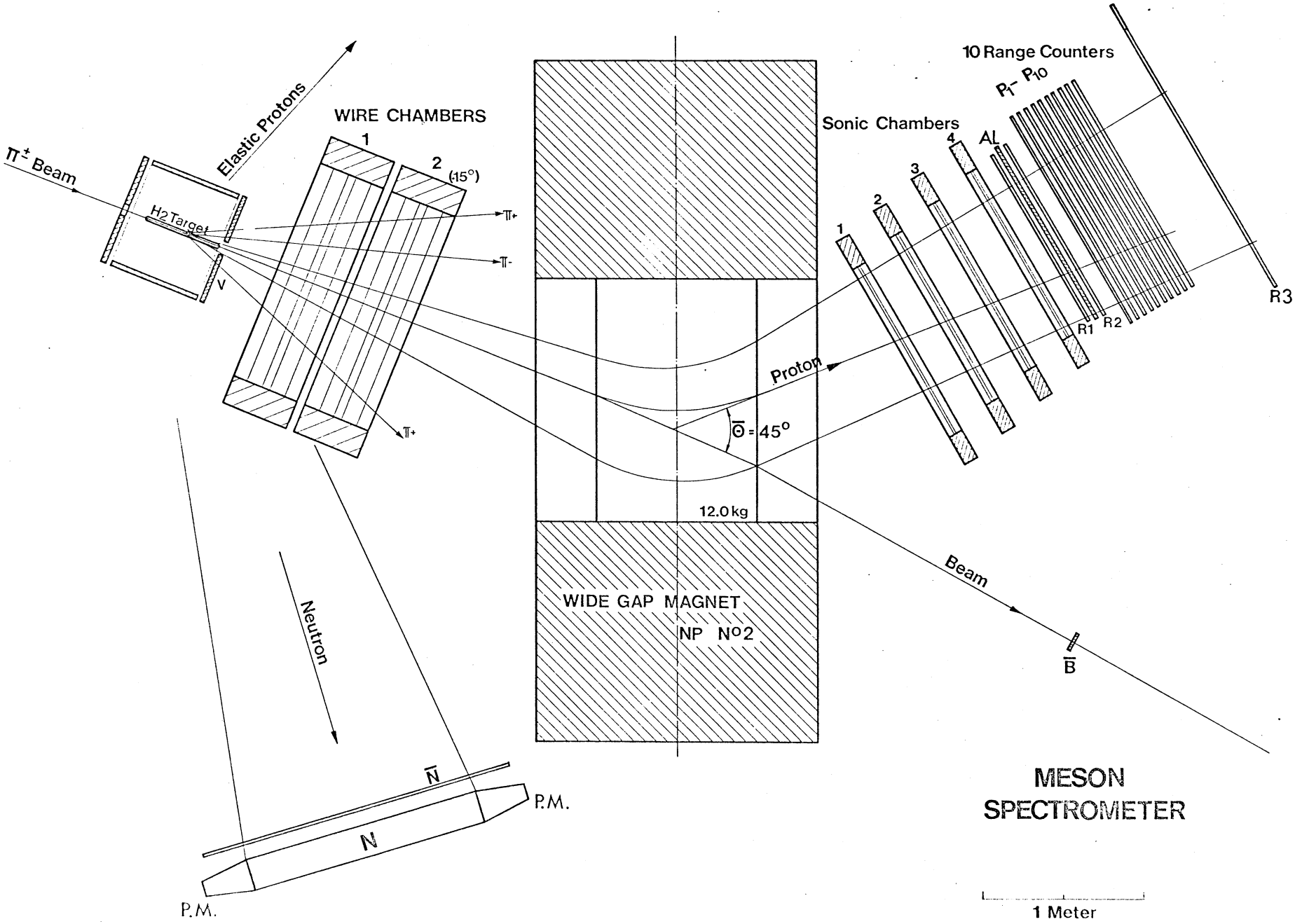
10 Range Counters
P_1 - P_{10}
Sonic Chambers
WIRE CHAMBERS
1
2
(15°)
Elastic Protons
$\pi^{\pm}$ Beam
H_2 Target
V
π^+
π^-
π^+
Proton
$\bar{\Theta}$ = 45°
12.0 kg
WIDE GAP MAGNET
NP N°2
Beam
$\bar{B}$
Neutron
$\bar{N}$
N
P.M.
P.M.
AL
R1
R2
R3
MESON
SPECTROMETER
1 Meter

FIG. 2

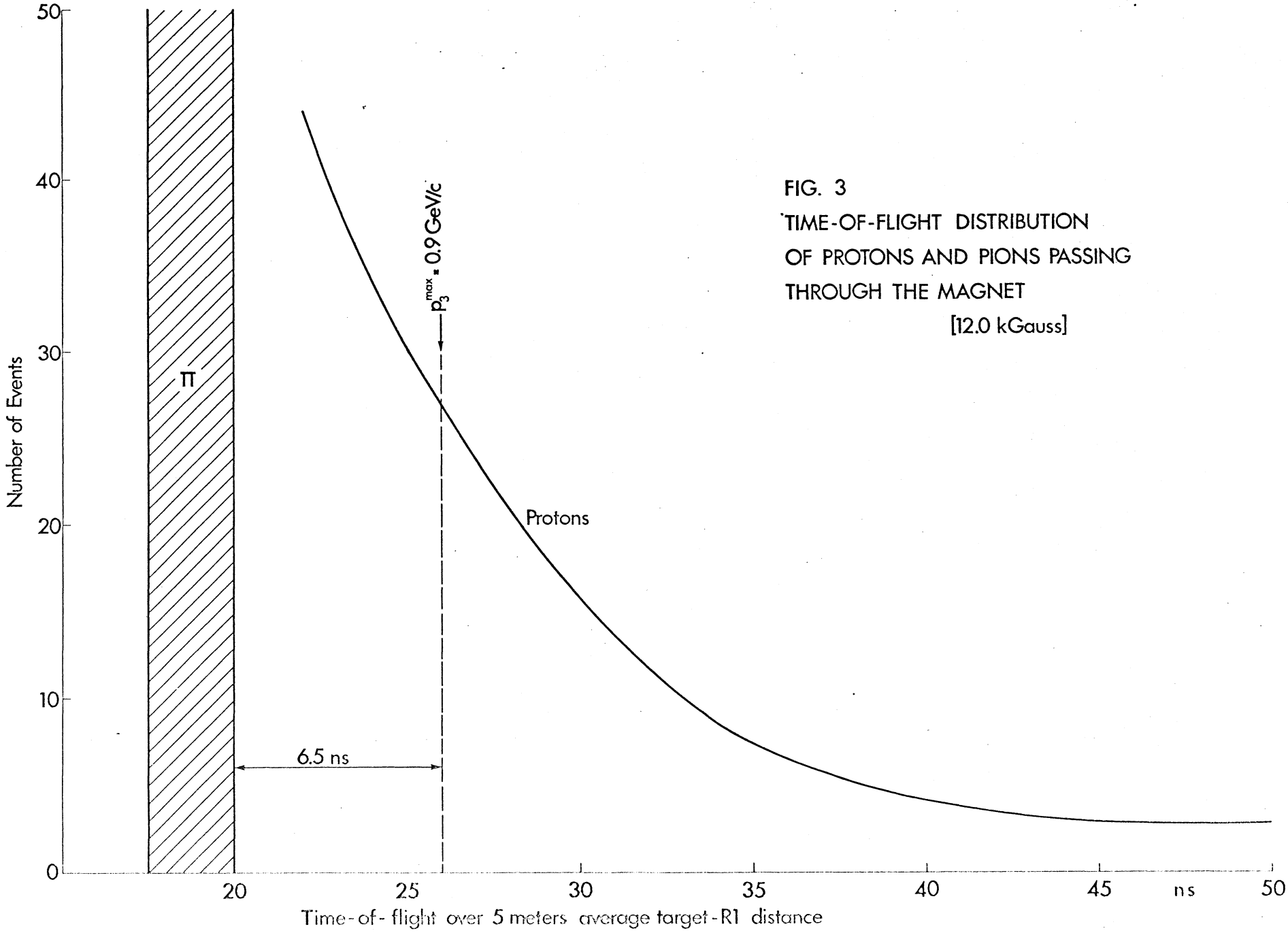

FIG. 3
TIME-OF-FLIGHT DISTRIBUTION
OF PROTONS AND PIONS PASSING
THROUGH THE MAGNET
[12.0 kGauss]

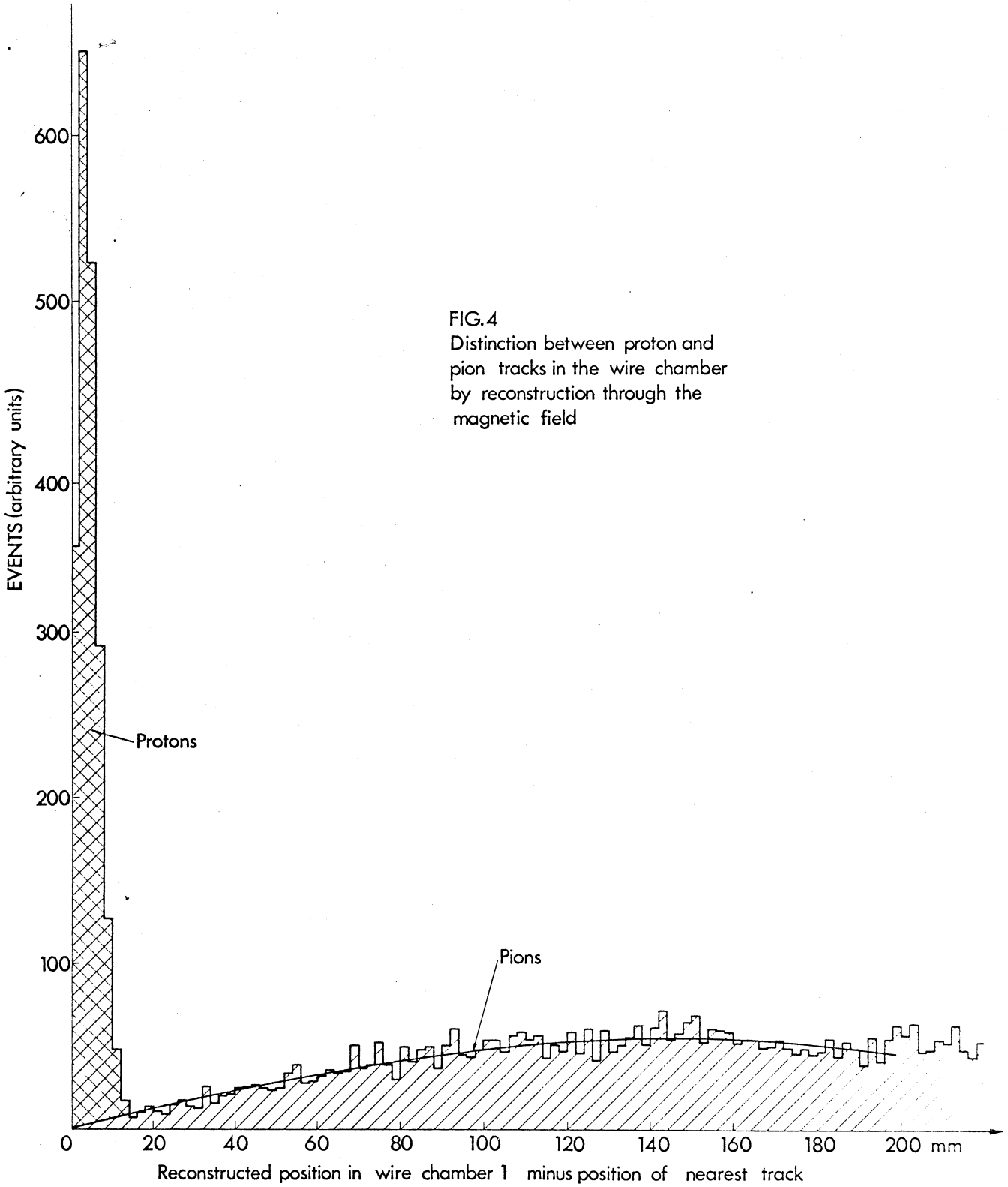

FIG. 4
Distinction between proton and pion tracks in the wire chamber by reconstruction through the magnetic field

fig. 5
TRANSMISSION FUNCTION
OF THE PROTON SPECTROMETER
FOR FLAT INPUT MASS SPECTRUM

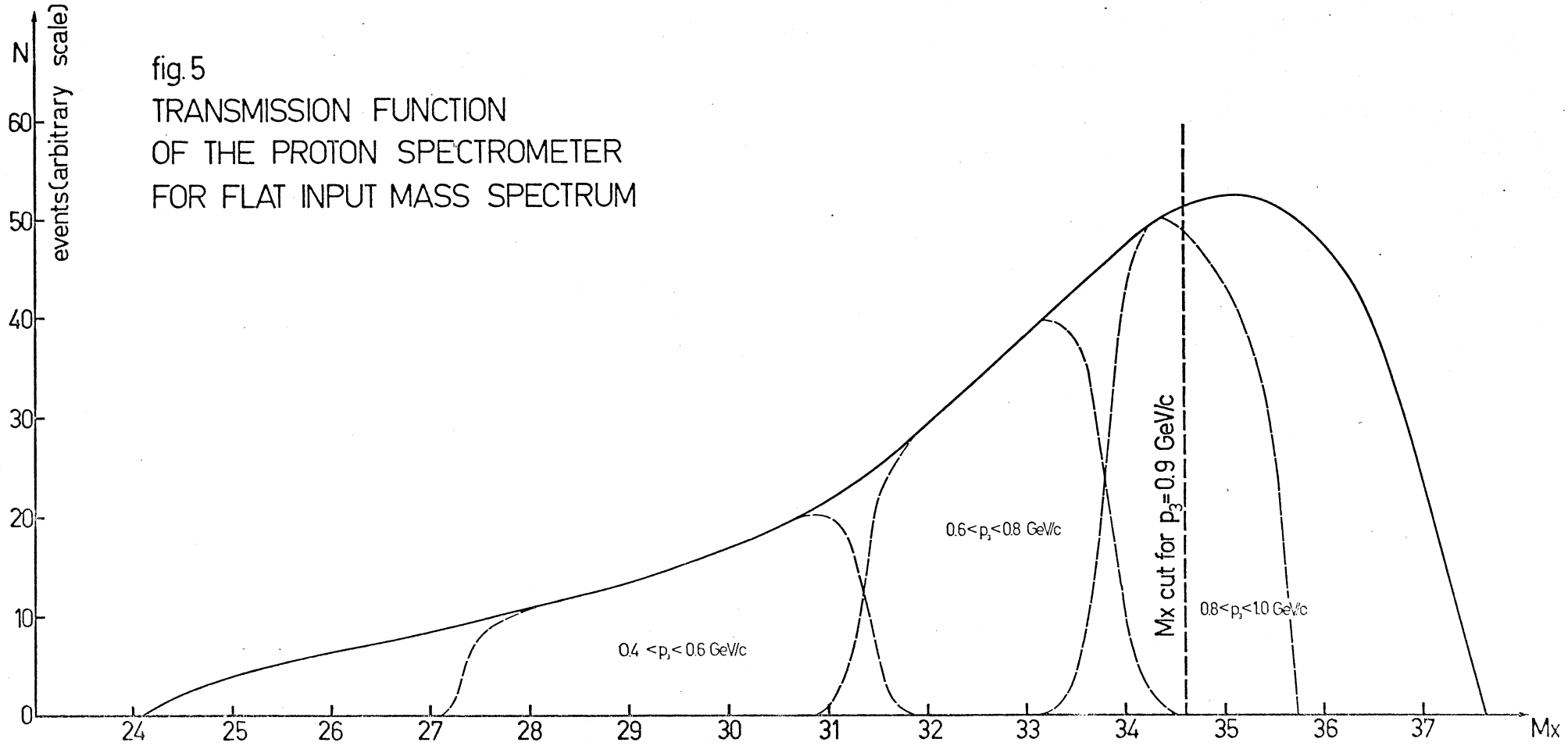

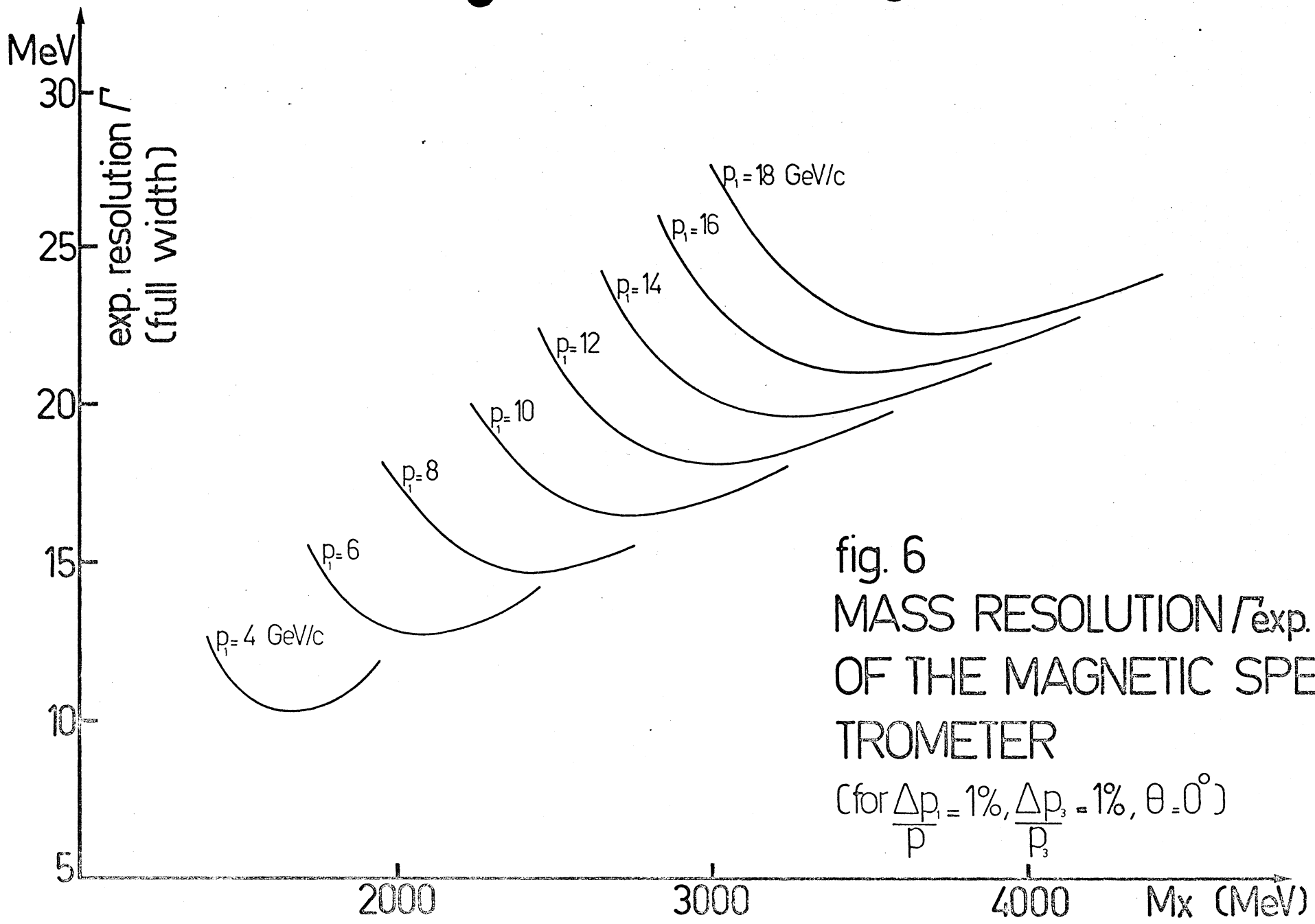

fig. 6
MASS RESOLUTION $\Gamma_{exp.}$ OF THE MAGNETIC SPECTROMETER
(for $\frac{\Delta p_1}{p} = 1\%$, $\frac{\Delta p_3}{p_3} = 1\%$, $\theta = 0^\circ$)

fig. 7

ACCEPTANCE OF THE WIRE CHAMBERS AS FUNCTION OF Mx AND P1 FOR X^- DECAYING INTO 3 CHARGED PIONS

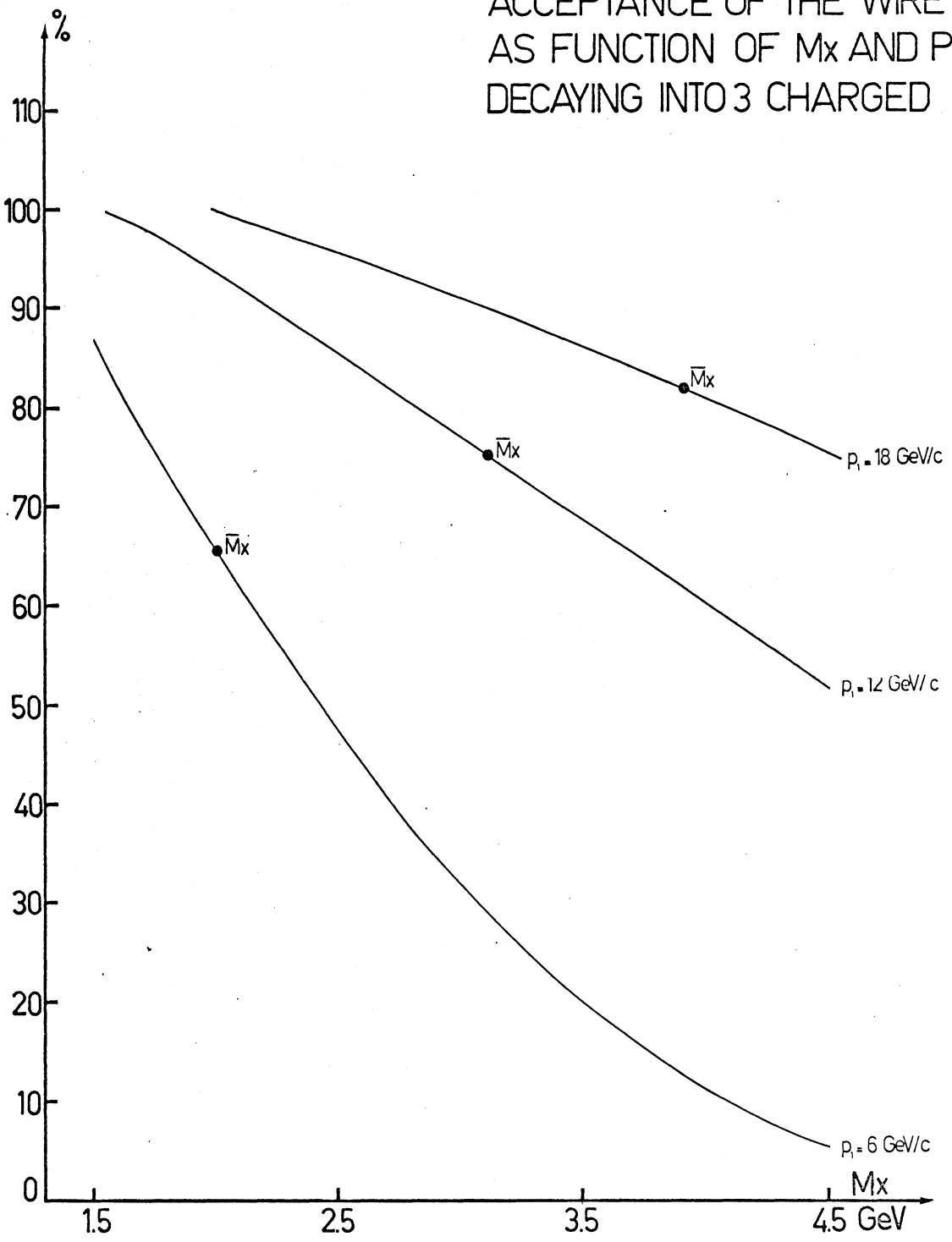

fig. 8

DIFFERENCE BETWEEN MISSING MASS AND EFFECTIVE MASS

A2 run, 7 GeV/c, January 1967

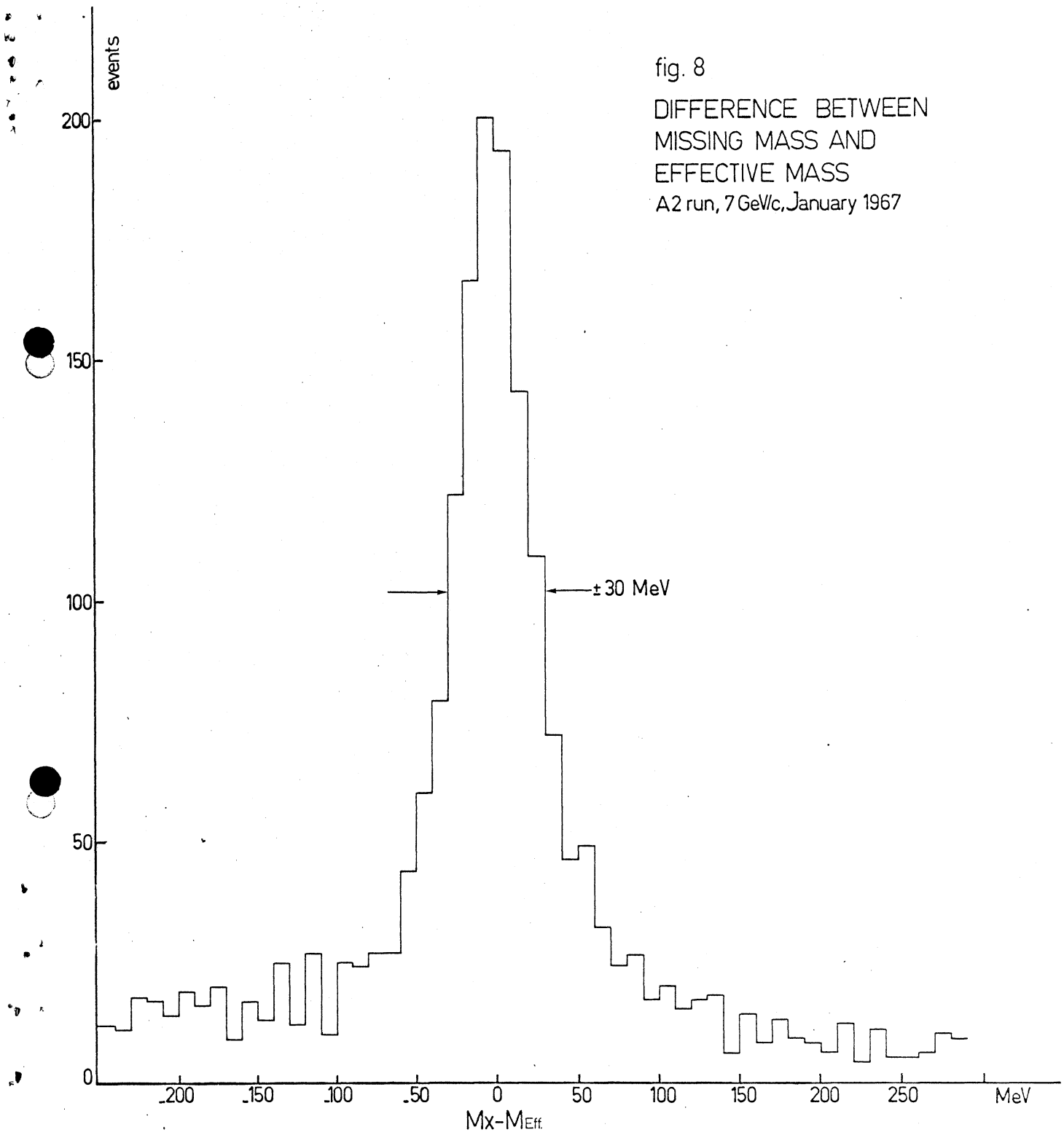

fig. 9a

FAST LOGICS (schematic)

TRIGGER CONDITION

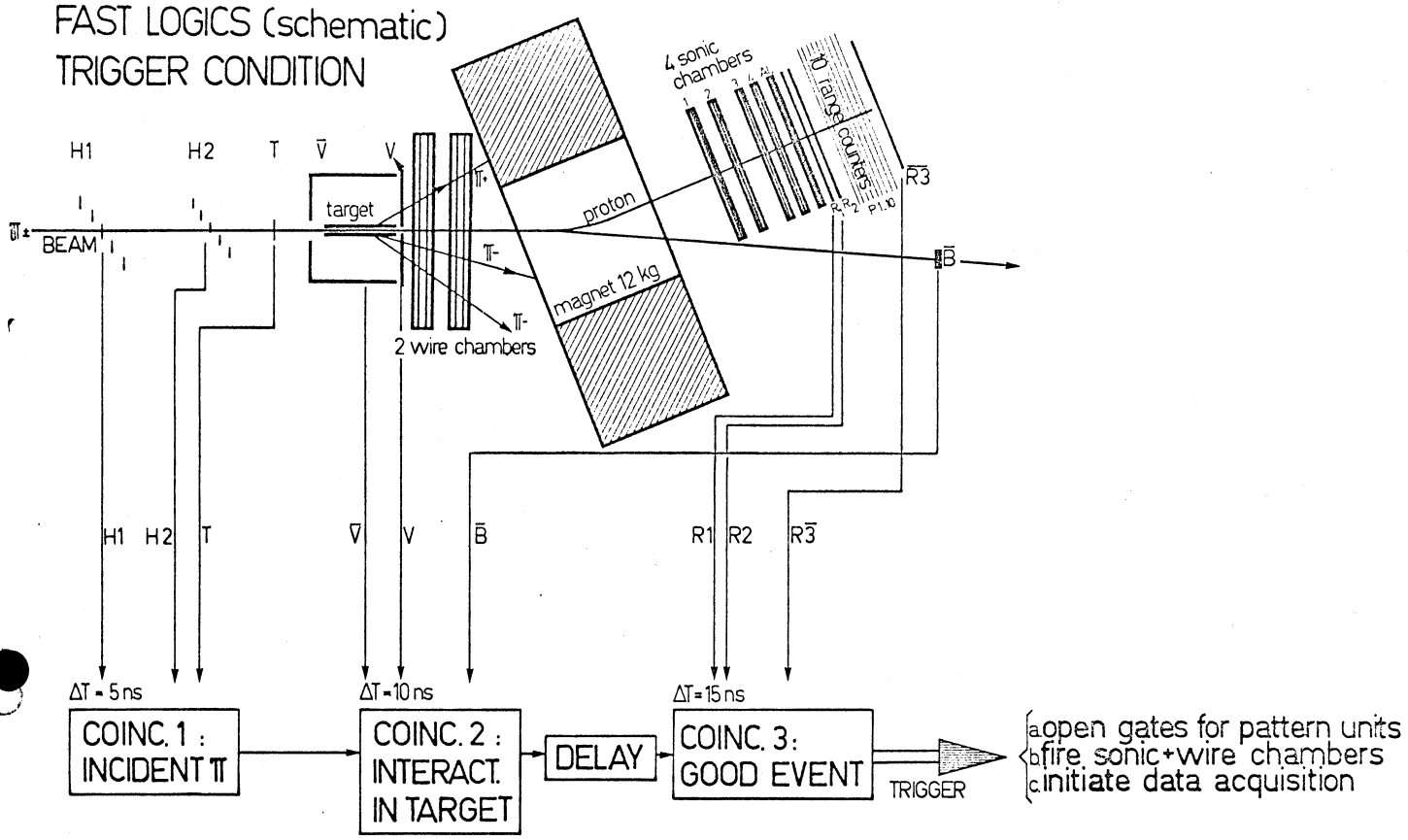

Full trigger requirement :
H1 H2 T V V̄B̄ R1 R2 R̄3

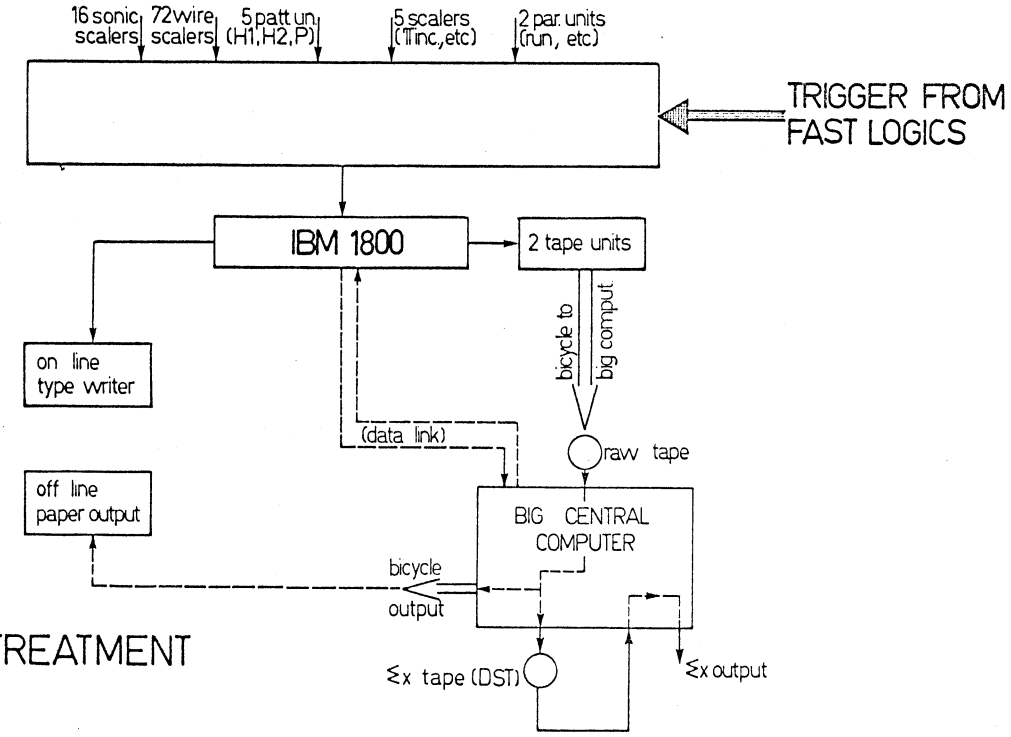

fig. 9b

DATA TREATMENT